

CFD-response surface methodology to optimize the effective thermal conductivity and homogeneity in tray dryer

CFD acoplada a la metodología de superficie de respuesta para optimizar la conductividad térmica efectiva y la homogeneidad en un secador de bandejas

Hugo Fabian Lobatón-García^{1*} ; Natali López-Mejía¹ ; Wilmer Cruz-Guayacundo² 

¹Universitaria Agustiniiana. Bogotá, D.C., Colombia; e-mail: hugo.lobaton@uniagustiniana.edu.co, natali.lopez@uniagustiniana.edu.co.

²Universitaria Agustiniiana, Facultad de Ingeniería. Bogotá, D.C., Colombia; email: wilmer.cruz@uniagustiniana.edu.co

*corresponding author: hugo.lobaton@uniagustiniana.edu.co

How to cite: Lobatón-García, H.F.; López-Mejía, N.; Cruz-Guayacundo, W. 2023. CFD-response surface methodology to optimize the effective thermal conductivity and homogeneity in tray dryer. Rev. U.D.C.A Act. & Div. Cient. 26(2):e2241. <http://doi.org/10.31910/rudca.v26.n2.2023.2241>

Open access article published by Revista U.D.C.A Actualidad & Divulgación Científica, under Creative Commons License CC BY-NC 4.0

Official publication of the Universidad de Ciencias Aplicadas y Ambientales U.D.C.A, University, Accredited as a High-Quality Institution by the Colombian Ministry of Education.

Received: March 14, 2022

Accepted: July 17, 2023

Edited by: Rita María Ávila G. de Hernández

ABSTRACT

Tray dryers are usually designed with simplistic scaling rules that do not account for all the transport phenomena associated with drying. The use of computational fluid dynamics coupled with response surface methodology can be a powerful tool to evaluate how different tray dryer design parameters affect the drying process. In this work, two tray dryers, one with a lateral air inlet and another with a bottom air inlet, were parameterized for the position of the air inlet, the dryer length, and the distance between the trays. A central composite design was chosen to determine the sample points, and the average turbulence viscosity and effective thermal conductivity as well as the homogeneity index were calculated. With these values, a response surface curve was constructed. The effective thermal conductivity and its homogeneity index were improved (80 % and 11 %, respectively) with an increased distance between trays and an air inlet located in the middle of the inlet face in the best scenario. In addition, the reductions in effective thermal conductivity outcomes were minimal due to the scale-up process in terms of the dryer length.

Keywords: Effective thermal conductivity; Food preservation; Postharvest processes; Preservation techniques; Tray dryer design.

RESUMEN

Los secadores de bandejas se suelen diseñar con reglas de escala simplistas, que no tienen en cuenta todos los fenómenos de transporte, asociados con el secado. El uso de dinámica de fluidos

computacional junto con la metodología de superficie de respuesta puede ser una herramienta poderosa, para evaluar cómo los diferentes parámetros de diseño del secador de bandeja afectan el proceso de secado. En este trabajo se parametrizaron dos secadores de bandeja, uno con entrada de aire lateral y otro con entrada de aire inferior, variando la posición de la entrada de aire, la longitud del secador y la distancia entre las bandejas. Se eligió un diseño compuesto central, para determinar los puntos de muestra y se calcularon la viscosidad de turbulencia promedio y la conductividad térmica efectiva, así como el índice de homogeneidad. Con estos valores se construyó una curva de superficie de respuesta. Se mejoró la conductividad térmica efectiva y su índice de homogeneidad (80 y 11 %, respectivamente), con una mayor distancia entre platos y una entrada de aire, ubicada en el medio de la cara de entrada en el mejor escenario. Además, las reducciones en los resultados de la conductividad térmica efectiva fueron mínimas, debido al proceso de ampliación en términos de la longitud del secador.

Palabras clave: Conductividad térmica efectiva; Conservación de alimentos; Diseño de secador de bandejas; Procesos de poscosecha; Técnicas de conservación.

INTRODUCTION

Colombia has been identified as an agricultural country with a great variety of biological material. This country produces diverse fruits, vegetables, medicinal plants and, recently, nutraceuticals, such as microalgae, for local consumption and export. This activity

is mainly concentrated in rural areas, where the transportation and energy infrastructures in some regions are inadequate, leading to a reduction in crop quality (Subramaniam, 2016). In addition, the struggle to access new and efficient conservation technology limits farmers' options in preserving crop quality. Drying operations, cold chains, and microbial disinfection, among other postharvest processes, are necessary to increase the shelf life of biological materials once they are harvested (Subramaniam, 2016). However, it has been reported that due to nonoptimal equipment designs, the energy consumption of these operations is high, and the quality of the final product is usually compromised (Salami *et al.* 2010). The design of agro-industrial equipment that extends the useful life of biological products as dryer, and cold rooms is typically implemented with empirical correlations or simply based on practical knowledge bases that, though significant, often omit important phenomena. Therefore, these devices are inefficient in both energy use and unit operation performance, which can affect the final quality of the product (Precoppe *et al.* 2015). Air distribution in dryers should be addressed in different ways, to fill the design, optimization and scale up gap.

With the emergence of higher computational efficiencies, it is now possible to use computational fluid dynamics to solve problems involving mass, energy, and momentum transport equations in computer aided design (Parpas *et al.* 2018). Although computational fluid dynamics - CFD has been widely used in the automotive and aerospace industries, its use has been limited in agroindustry. Moreover, coupling CFD with the design of experiments - DOE method that is normally applied for *in vivo* checks can generate complete integration in computer aided design when coupled with *in silico* experiments.

For example, the coupling between response surface methodology - RSM and CFD has recently been used in the optimization of solar heaters (Qader *et al.* 2019), miscible liquid mixers (Mansour *et al.* 2020), and bubble columns (Gholamzadehdevin & Pakzad, 2019). The coupling of CFD with the design of factorial type experiments has also been reported to study the relationships among the configuration of a ring baffle (Samruamphianskun *et al.* 2012), the hydrodynamic phenomena of a reactor and the use of response surfaces in the design of cooling microchannels (Bal *et al.* 2018). Recently, CFD coupled with RSM was used to determine the optimal geometry parameters that maximize the Nusselt number and minimize the friction factor in a double-pipe heat exchanger (Arjmandi *et al.* 2020).

Drying is the main food preservation method used in developing countries (Nema *et al.* 2015), and although there are promising drying technologies (Figiel & Michalska, 2017), nearly 85 % of industrial dryers are convective, with hot air used as a drying medium (tray dryer). This is due to the simple design, low construction cost and capacity of convective dryers to dry products at high volume (Darabi *et al.* 2015). The influences of relative humidity and air velocity on the drying process are key factors in the energy reductions responsible for an estimated 15 to 20 % of industrial energy use (Ndisya *et al.* 2020). Indeed, the improper

distribution of air inside a drying chamber can lead to inefficient and nonuniform drying. Hot air is usually introduced near the first tray and passes over other trays; therefore, some trays have superior air flows compared to others due to pressure losses, resulting in a biological material with a heterogeneous final humidity. In addition, increments in air velocity used to solve this problem lead to higher energy costs (Tzempelikos *et al.* 2012). These issues have been reported in convective dryers in both simulations and experimental validations; however, due to their low manufacturing cost, they are still widely used in developing countries (Esparza E. *et al.* 2019; Precoppe *et al.* 2015; Vargas *et al.* 2018).

Traditional kinetics models do not account for the influence of flow and transport properties, which are based on the geometrical configurations and operating parameters of tray dryers (Chilka & Ranade, 2018). Therefore, 3D models of dryers have been created in CFD and experimentally validated by several researchers. With this powerful tool, it is now possible to check for nonhomogeneous spatial distributions of variables such as turbulence viscosity (μ_t), the turbulent transfer of momentum by eddies giving rise to an internal fluid friction or effective thermal conductivity (k_{eff}), a measure of a material's ability to transfer energy; however, this information has to be linked to the drying kinetics (Subramaniam, 2016) to obtain a more robust model that can predict spatial humidity. Once a completed model has been developed, it is even possible to integrate physical models with multi-objective optimization processes to achieve a complete integration of computer-assisted dryer design (Defraeye, 2014). With a CFD model, local values of turbulence viscosity and effective thermal conductivity can be calculated (Böhner *et al.* 2013; Tzempelikos *et al.* 2012; Vargas *et al.* 2018) and the variations in values can be estimated with a uniformity index. For example, Khatir *et al.* (2013) set a temperature uniformity index for CFD optimization of a commercial bread-baking oven, and Precoppe *et al.* (2015) showed a uniformity index for local velocities in a tray dryer. In this study, a CFD tray dryer model is coupled with a DOE method and surface response methodology to determine optimal geometric parameters (distance between the trays, air inlet position and dryer length) and improve turbulence viscosity, effective thermal conductivity, and uniformity in the dryer.

MATERIALS AND METHODS

Mathematical model and numerical simulation. The momentum and continuity equations were set for the air as follows (ANSYS, 2017):

$$\frac{\partial \rho}{\partial t} + \nabla \cdot (\rho \vec{v}) = 0 \quad \text{equation 1}$$

$$\frac{\partial \rho \vec{v}}{\partial t} + \nabla \cdot (\rho \vec{v} \vec{v}) = -\nabla \cdot P + \nabla \cdot (\bar{\tau}) + \rho g \quad \text{equation 2}$$

$$\frac{\partial \rho}{\partial t} + \nabla \cdot (\rho \vec{v}) = 0 \quad \text{equation 3}$$

$$\mu_t = \rho c_u \frac{\kappa^2}{\varepsilon} \quad \text{equation 4}$$

Where, ρ is the density of air (kg/m^3); t is the time (s), \vec{v} is the velocity (m/s); $\bar{\tau}$ is the tensor and μ_t is the turbulent viscosity (Pa s); c_n is the turbulence model constant.

The k- ϵ model was used to model the turbulence (ANSYS, 2017). This model has been proven to be efficient in turbulence modeling for tray dryers (Dasore & Konijeti, 2019; Margaris & Ghiaus, 2006):

$$\frac{\partial \rho k}{\partial t} + \nabla \cdot (\rho \vec{v} k) = \nabla \cdot \left(\mu + \frac{\mu_t}{\sigma_k} \right) + G + \rho \epsilon \quad \text{equation 5}$$

$$\frac{\partial \rho \epsilon}{\partial t} + \nabla \cdot (\rho \vec{v} \epsilon) = \nabla \cdot \left(\mu + \frac{\mu_t}{\sigma_\epsilon} \right) + C_1 \frac{\epsilon}{k} G - C_2 \frac{\epsilon^2}{k} \quad \text{equation 6}$$

The modeled energy equation is:

$$\frac{\partial T}{\partial t} + \nabla \cdot (\rho \vec{v} C_p T) = \nabla \cdot (k_{eff} \nabla T) \quad \text{equation 7}$$

Where, (K_{eff}) is the Effective thermal conductivity (W/ m k); C_1 C_2 C_3 is the Turbulence model constant; G is the production of turbulence kinetic energy; T is temperature ($^\circ\text{C}$).

For k- ϵ model the effective thermal conductivity is given by:

$$k_{eff} = K + \frac{C_p \mu_t}{Pr_t} \quad \text{equation 8}$$

Where in this case, is the thermal conductivity (. The default value of the turbulent Prandtl (Pr_t) (number is 0.85. Equation 8 shows the relationship between turbulent viscosity and thermal effective coefficient. The higher the turbulent viscosity, the higher the thermal effective coefficient.

The model constants have the following default values: $C_{\mu}=0,09$, $C_1=1,44$, $C_2=1.92$ and $\sigma_k=1$ $\sigma_\epsilon=1.3$.

The air thermal properties were, density 1.225 (kg/m^3), cp 1006.43 (J/kg.K), thermal conductivity 0.0242 (W/m.K), viscosity $1.78e^{-5}$ (Kg/m.s)

The boundary conditions were the velocity inlet for the air inlet and the pressure outlet for the air outlet. A no-slip boundary condition was used for all the walls. All models were solved with Fluent-ANSYS software (using second-order upwind methods and a coupled pressure-velocity scheme). The COUPLE algorithm was used alongside a Fluent solver to solve the pressure-velocity coupling equations 1 and 2 (ANSYS, 2017). The numerical model was run until it converged. The simulation strategy was 300 hundred interactions, residuals $1 e^{-3}$ quick algorithm was used to solve turbulent and energy equations.

Prior to the tray dryer parameterization, the model was validated against the local velocities measured for conditions and a tray dryer presented by Tzempelikos *et al.* (2012).

Original tray dryer geometry. The original tray dryer (Figure 1a) consists of a rectangular aluminium chamber with dimensions of 873 mm (length) x 545 mm (width) x 1310 mm (height). The

dryer has an air inlet located at the bottom of the left side face, which has a turbine that is responsible for circulating air from the outside to the inside with a resistance system for heating the air that enters the chamber. The diameter of the duct is 109 mm. Additionally, a camera with an air outlet is located at the upper part of the right lateral face. The cabinet has 10 fixed aluminium trays that are 94.44 mm apart (dimensions of each tray are 581 mm x 500 mm) for a drying area of 2.92 m^2 . Homogeneity problems were previously described in this type of dryer, where different final humidities were obtained at the spatial level for equal drying times (Esparza E. *et al.* 2019).

In addition to the original tray dryer, two additional dryers were parameterized: a dryer with a lateral inlet TDLI (Figure 1b) and a dryer with a bottom inlet TDBI (Figure 1c) The dryers were parameterized with three design variables: the position of the air inlet, the distance between the trays and the dryer length.

Position of the air inlet - Pinlet ranges from 0 (initial position) to 900 mm. Dryer length (L) ranges from 0 (initial position) to 500 mm, and distance between the trays (h) ranges from 100 to 450 mm. These values were chosen as the maximum values due to the construction constraints. It is important to note that when h changes, the number of trays changes automatically to meet the desired h , which will be explained later in detail in this document. Ansys 2017 R1 (Student version) was used to create the geometry and the mesh.

Response variable. The response variables in this work are (μ_t), (K_{eff}) (and its uniformity index γ , (μ_t) and (K_{eff}) (is the average of the turbulence viscosity and effective thermal conductivity of all nodes, which are calculated with equation 4 and with equation 8 for each node.

Esparza E. *et al.* (2019) demonstrated with experiments and simulations that variations in k_{eff} directly affect drying speed. Spatial variations for these variables create nonhomogeneity during the drying process. To quantify these variations, the uniformity index of the effective thermal conductivity is established, which shows the variation of a variable in space, where a value of 1 means maximum uniformity. The uniformity index (ANSYS, 2017) is calculated using the equation below, where ϕ_i is the value of the effective thermal conductivity at a point and A_i is the total volume where the variable is being evaluated. The analysis volume was defined in the space where the trays are located, as shown in figure 1.

$$\gamma = 1 - \frac{\sum_{i=1}^n \left[\left(\left| \phi_i - \frac{k_{eff}}{k_{eff}} \right| \right) \times A_i \right]}{2 \times \left| k_{eff} \right| \times \sum_{i=1}^n A_i} \quad \text{equation 9}$$

Experimental design and optimization. The dryer was parameterized with three design variables: the position of the air inlet, the distance between the trays and the dryer length. The sample points of these parameters were chosen by using central composite design. Central composite design - CCD is based on 2-level factorial designs augmented with centre and axial points

to fit quadratic models. Regular CCDs have 5 levels for each factor (Arjmandi *et al.* 2020). Table 1 shows the sample points for which the response variable is calculated. Working with this type of experimental design, the sample points not only reduce the number of points required but also increase the accuracy of the response surface. For all sample points, the inlet velocity was fixed to 3 ms^{-1} . With the values calculated with the CFD code, a surface is generated. Genetic aggregation is the default algorithm

used to generate response surfaces. It automates the process of selecting, configuring, and generating the type of response surface best suited for each output parameter (ANSYS, 2017). Finally, the optimization is carried out by setting the objective function based on the generated response curve. In this work, the objective was to maximize the turbulent viscosity, effective thermal conductivity, and its uniformity index.

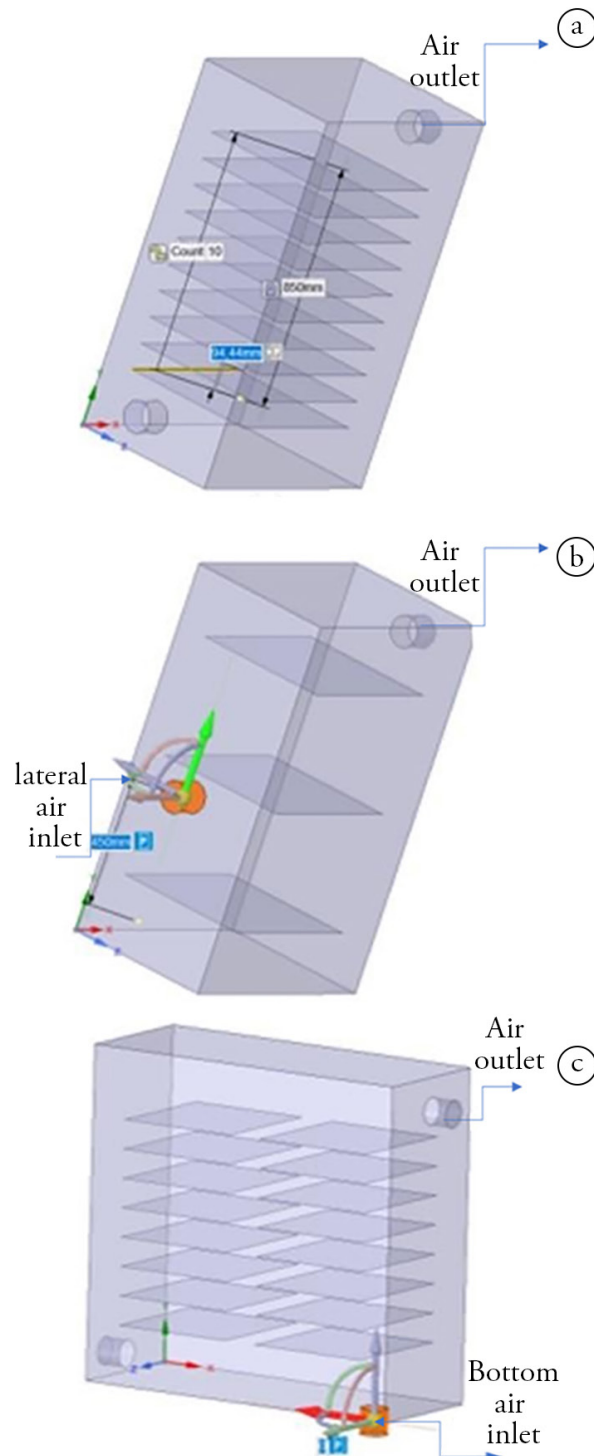


Figure 1. Tray Dryer Modeling (Geometry). a) original tray dryer; b) dryer with a lateral inlet (TDLI); c) dryer with a bottom inlet (TDBI).

Table 1. Experimental design and results for the tray dryer with a lateral air inlet (TDLI).

Sample point	Pinlet (mm)	L (mm)	h (mm)	μ_t (Pa . s)	k_{eff} (W /m k)	γ
1	450	250	275	0.00182	2.13	0.70563
2	0	250	275	0.00151	1.80	0.63979
3	900	250	275	0.00162	1.94	0.67613
4	450	0	275	0.00186	2.22	0.72716
5	450	500	275	0.00182	2.20	0.68487
6	450	250	100	0.00105	1.24	0.67830
7	450	250	450	0.00176	2.07	0.71913
8	84	47	133	0.00136	1.63	0.63116
9	816	47	133	0.00138	1.65	0.69378
10	84	453	133	0.00123	1.46	0.56299
11	816	453	133	0.00113	1.35	0.65516
12	84	47	417	0.00192	2.29	0.71140
13	816	47	417	0.00185	2.21	0.69852
14	84	453	417	0.00184	2.20	0.64878
15	816	453	417	0.00195	2.30	0.67305

K_{eff} : Effective thermal conductivity. Pinlet: Position of the air inlet. L: Dryer length; h: Distance between the trays γ : Uniformity index.

RESULTS AND DISCUSSION

Table 1 shows the μ_t , K_{eff} and γ results for all the design points analysed in the TDLI (TDBI also has an experimental design; however, data is not presented). Point 4, 7 and 12 show the best values regarding turbulence (the selected points were those with which the highest values of turbulence, thermal conductivity and uniformity index were simultaneously obtained) and effective thermal conductivity due to the linear relationship between turbulence and effective thermal conductivity (Figure 2a). Likewise, these points show the highest uniformity index values. To better understand the behaviour of turbulence and uniformity, these data are used to construct the response surface. Figure 2b shows the behaviour of effective thermal conductivity and uniformity with respect to h value and length at a fixed value of 450 mm for Pinlet. The effective thermal conductivity values and the uniformity increase with increasing increments in the distance between trays (Figure 2c). However, increased increments in the distance between trays means a smaller number of trays. In addition, these graphs also show that for a constant value of h, the uniformity is reduced, but the effective thermal conductivity is barely affected by the increment in tray dryer length (Figure 3b). These findings are important criteria in the design and scale-up of tray dryers, as shown later in this document.

Figures 4a and 5a show the effective thermal conductivity and uniformity performance related to Pinlet and h for the dryer with a lateral inlet with a constant length of 500 mm. In this case, h also has a strong effect on turbulence. The increments in h enhance

effective thermal conductivity and uniformity. In addition, the lateral inlet at position zero (original position) shows poor uniformity and effective thermal conductivity values (blue zones in the surface graphic). These results imply that the current position of the inlet in the original dryer does not maximize effective thermal conductivity.

For the equipment with the air inlet located at the bottom inlet, the inlet position becomes more relevant in relation to the effective thermal conductivity (Figure 2c). The maximum effective thermal conductivity value is found when the position is in the middle of the bottom wall of the dryer. Conversely, uniformity is negatively affected when the input position is in the middle (Figure 3d). The results of this work show that elements that interrupt flow decrease turbulence and effective thermal conductivity but increase homogeneity. Tzempelikos *et al.* (2012) found reductions in turbulence values due to trays that drastically interrupt the flow.

A turbulent flow around the food matrix improves the mass and heat transfer in the layer that is formed around the food material (Sabarez, 2016). It is important to note that turbulence is an important factor affecting the drying rate during the external heat and mass transfer controlling phases (Sabarez, 2016). Beyhaghi *et al.* (2016) and Lecorvaisier *et al.* (2010) found better diffusivity coefficients in turbulent flows than in laminar flows, showed that the drying time for a turbulent flow was less than that for a laminar flow, and the evaporation rate (or evaporative mass flow rate) was greater for a turbulent flow than a laminar flow.

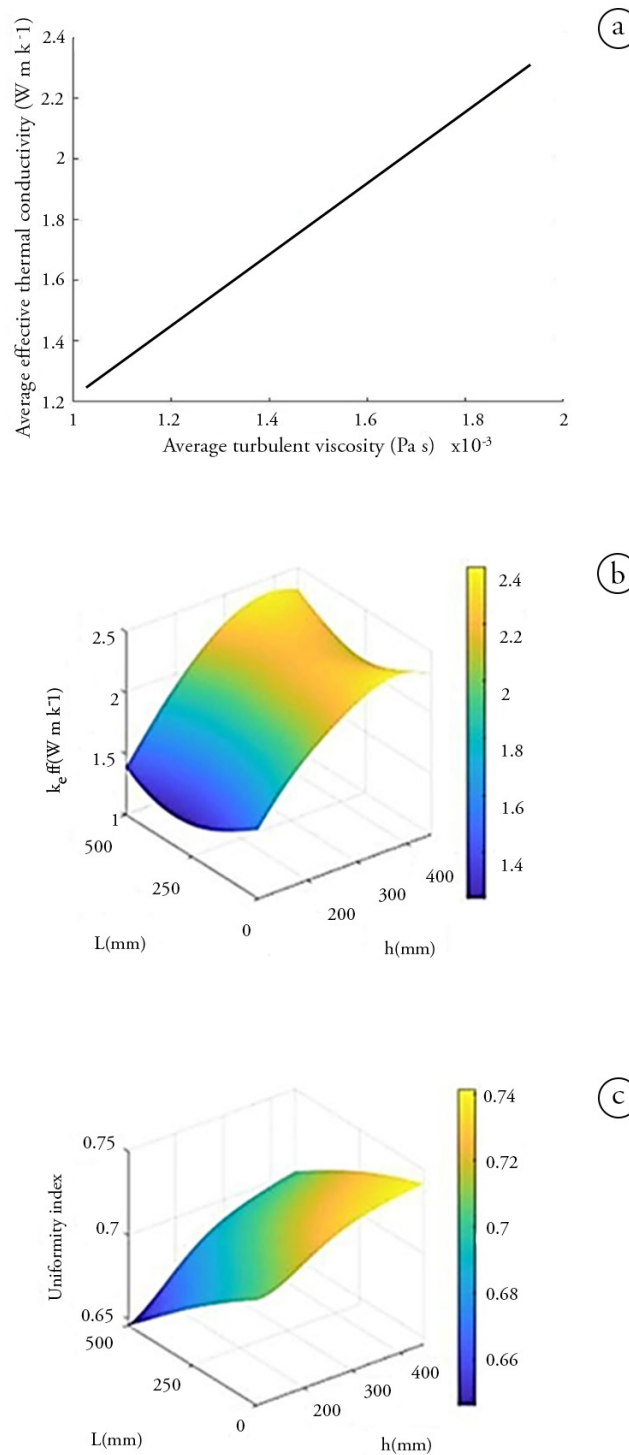


Figure 2. (a) Average turbulent viscosity vs Average effective thermal conductivity. Influence of L and h on effective thermal conductivity (b), and uniformity index (c). The position P_{inlet} is constant (450 mm) for the tray dryer lateral (TDLI).

As stated before, the decrease in turbulence and therefore effective thermal conductivity affects the drying speed, and an uneven distribution of effective thermal conductivity generates different drying speeds between the trays (Esparza E. *et al.* 2019). An increased increment of h creates a smaller number of trays. A value of h between 90 and 100 mm represents 10 trays, while a value

of 400 to 450 mm represents 3 trays. Having more trays implies a greater drying area; however, as this work shows, it also implies a reduction in the values related to turbulence, effective thermal conductivity, and uniformity. A trade-off between effective thermal conductivity, uniformity and drying area must be found.

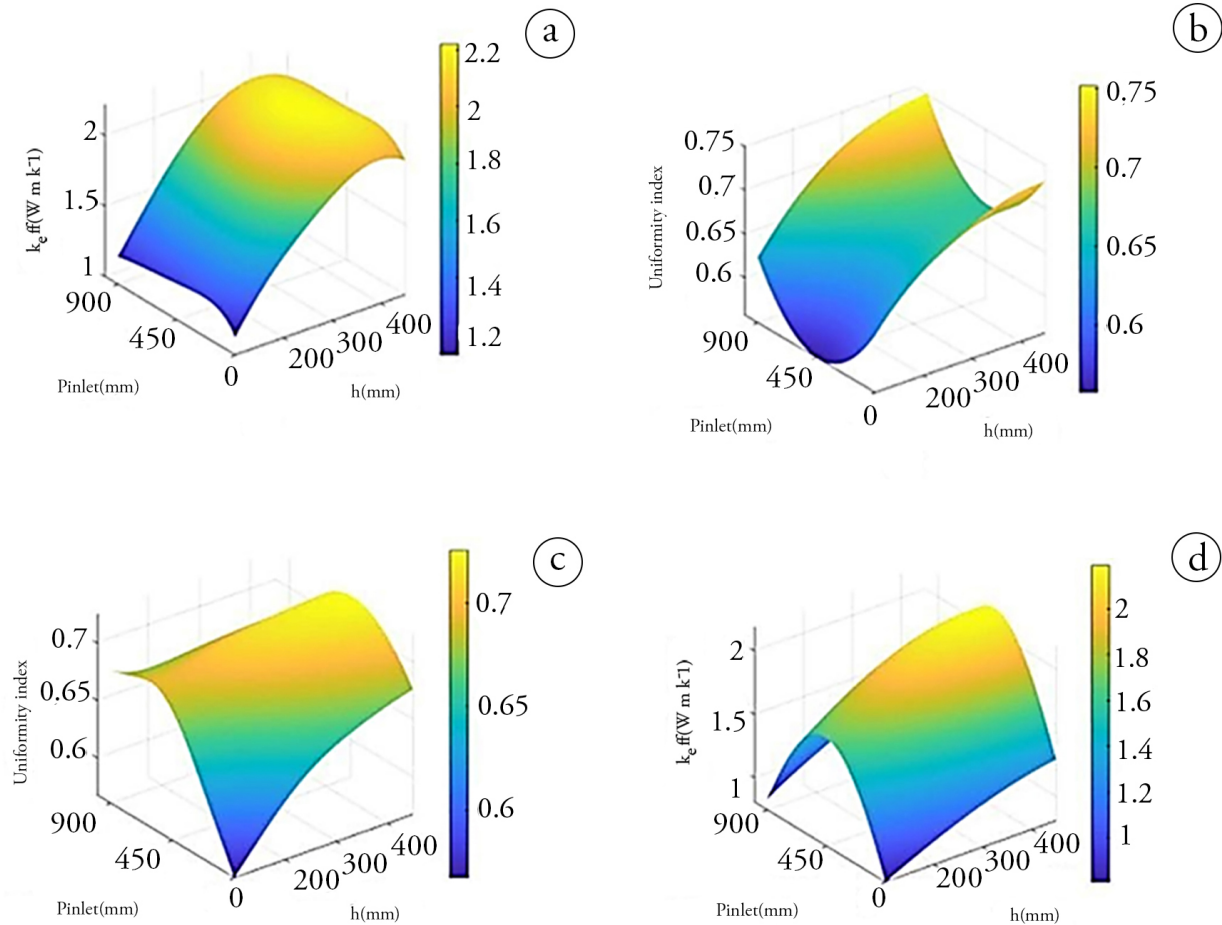


Figure 3. Influence of h and $Pinlet$ on effective thermal conductivity with a constant length of 500 mm: a) tray dryer lateral inlet (TDLI); b) tray dryer bottom inlet (TDBI). Influence of h and $Pinlet$ on uniformity with a constant length of 500 mm: b) tray dryer lateral inlet (TDLI); c) tray dryer bottom inlet (TDBI).

An objective function must be established carefully with specific constraints that a researcher can use to interpret the physical parameters of what constitutes an optimal design (Khatir *et al.* 2013). In this case, a large h means higher turbulence, effective thermal conductivity, and uniformity, but it also means fewer trays and therefore less drying area. However, with the findings related to the scale-up process, a comparison with similar drying areas can be performed. Table 2 shows the comparison of three configurations with respect to the original dryer. A 4-tray dryer with a width of 500 mm shows an 80 % increase in turbulence and effective thermal conductivity. However, it is a larger dryer and has a slightly smaller drying area than the original dryer. With the constraints on the drying area and knowing that increasing the length of the dryer means larger equipment, it is possible to determine the maximum surface curve. The optimal design for a dryer with a lateral inlet is an inlet position located in the middle, 500 mm larger than the original and a drying area of 2.13 m². This design shows an increase of 80 % in effective thermal conductivity and 11 % in uniformity compared to the original dryer. The optimal design of a tray dryer with a bottom inlet has the following conditions: an inlet position located in the middle, 500 mm larger than the original and a drying

area of 3.896 m². This design shows an increase of 40 % in effective thermal conductivity and a 4 % increment in uniformity compared to the original dryer.

Figure 4 shows the effective thermal conductivity isocontours in a plane located in the middle of the dryer for the 3 designs in table 2. This figure shows many red, yellow, and green areas in designs b and c compared with the original tray dryer. The challenge is to have most of the areas in the dryer exhibit yellow, green, and red areas inside the trays. As mentioned before, the zones with red colors (high turbulence and effective thermal conductivity) will have faster humidity removal rates.

Computer-aided design using CFD helps clarify the turbulence and effective thermal conductivity behavior in dryer equipment, and several works have shown the strong relationship between humidity removal and vigorous eddy viscosity to improve the mass transfer in the food boundary layer (Handayani *et al.* 2023). However, it is still necessary to correlate the findings in this theoretical research with empirical data, where the dryer design parameters can be modified experimentally, and the local humidity can be measured.

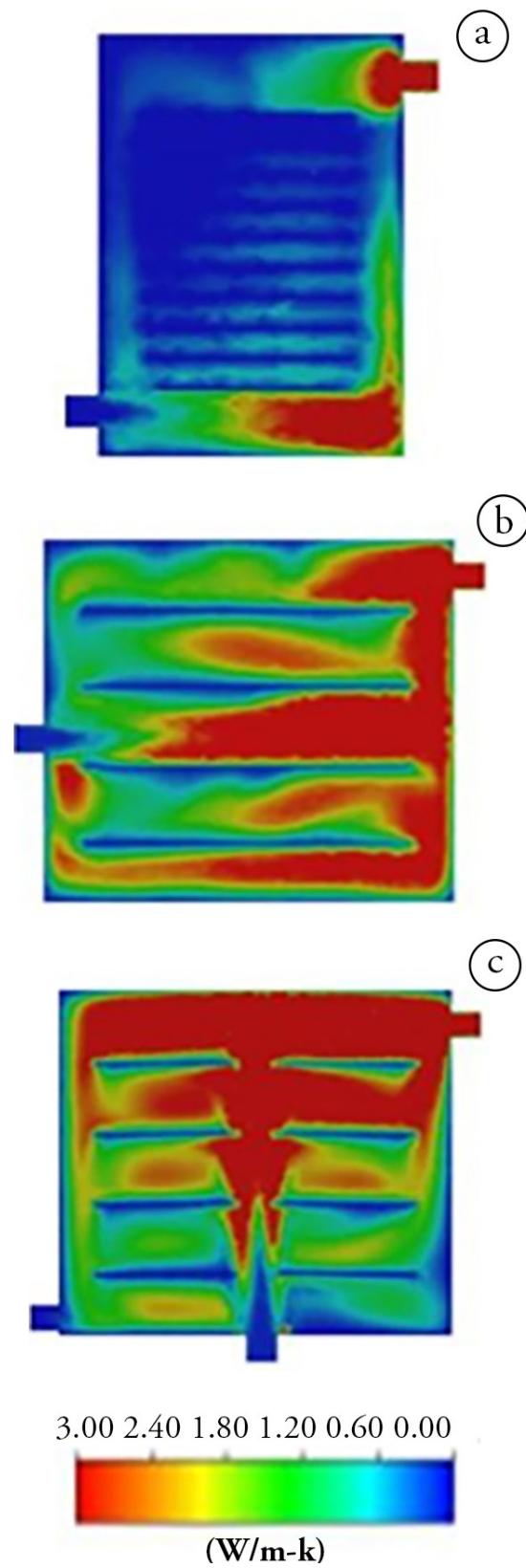


Figure 4. Effective thermal conductivity isocontours for different tray dryer configurations: a) Original tray dryer; b) TDLI 4 trays and c) TDLI 8 trays.

Table 2. Design parameters obtained for the analyzed geometries. Comparison between the original tray dryer with respect to the dryer with a lateral inlet (TDLI) and dryer with a bottom inlet (TDBI).

Parameter	Original tray dryer	TDLI	TDBI
Figure 1.	a	b	c
Number of trays	10	4	4 x 2
h (mm)	94	280	280
Drying area (m ²)	2.90	2.13	3.90
Pinlet (mm)	0.00	450.00	450.00
L (mm)	0.00	500.00	500.00
μ_t (Pa . s)	0.0011	0.0019	0.0017
k_{eff} (W/ m k)	1.3099	2.1954	2.0680
γ	0.6137	0.6885	0.6400

K_{eff} : Effective thermal conductivity. Pinlet: Position of the air inlet. L: Dryer length; h: Distance between the trays; γ : Uniformity index.

Finally, coupling experimental design with RSM can be a powerful tool for designing a tray dryer. In this case, design parameters such as dryer length, number of trays and inlet position were evaluated. A digital twin allows for a fast development design. Several design configurations can be evaluated before equipment construction and coupling with a design of experiments method, and an optimized number of runs can be found. This work shows that filling the dryer with many trays decreases the turbulence, effective thermal conductivity, and homogeneity; concerning the air inlet, the best effective thermal conductivity results are found when the air inlet is in the centre. Finally, the scale-up process regarding the dryer length increment shows small variations in effective thermal conductivity. These results present a new outcome regarding the tray dryer scale-up process.

Practical applications. This research shows an optimized dryer prototype using parameterization which can be used by the industry and by small producers who want to give added value to the products obtained from the field since it does not require a high investment for its implementation.

Acknowledgments. The authors thank the Universidad Agustiniiana for financing the INV-2020I1 project. **Conflicts of Interest:** The manuscript was prepared and revised by all authors, who declare the absence of any conflict which can put the validity of the presented results at risk. **Authors contribution.** Hugo Fabian Lobatón-García: Ideas; formulation or evolution of overarching research goals and aims. Preparation, creation and/or presentation of the published work. Natali López-Mejía: Synthesize study data. Writing – original draft Writing – review & editing. Wilmer Cruz-Guayacundo: Development or design of methodology; creation of models.

REFERENCES

1. ANSYS, INC. 2017. ANSYS Fluent Tutorial Guide. 1052p. Disponible desde Internet en: <http://users.abo.fi/rzevenho/ansys%20fluent%2018%20tutorial%20guide.pdf>
2. ARJMANDI, H.; AMIRI, P.; SAFFARI POUR, M. 2020. Geometric optimization of a double pipe heat exchanger with combined vortex generator and twisted tape: A CFD and response surface methodology (RSM) study. *Thermal Science and Engineering Progress.* 18:100514. <https://doi.org/10.1016/J.TSEP.2020.100514>
3. BAL, S.; MISHRA, P.C.; SATAPATHY, A.K. 2018. Optimization of spray parameters for effective microchannel cooling using surface response methodology. *International Journal of Heat and Technology.* 36(3):973-980. <https://doi.org/10.18280/IJHT.360325>
4. BEYHAGHI, S.; XU, Z.; PILLAI, K.M. 2016. Achieving the inside-outside coupling during network simulation of isothermal drying of a porous medium in a turbulent flow. *Transport in Porous Media.* 114:823-842. <https://doi.org/10.1007/s11242-016-0746-3>
5. BÖHNER, M.; BARFUSS, I.; HEINDL, A.; MÜLLER, J. 2013. Improving the airflow distribution in a multi-belt conveyor dryer for spice plants by modifications based on computational fluid dynamics. *Biosystems Engineering.* 115(3):339-345. <https://doi.org/10.1016/J.BIOSYSTEMSENG.2013.03.012>
6. CHILKA, A.G.; RANADE, V.V. 2018. CFD modelling of almond drying in a tray dryer. *The Canadian Journal of Chemical Engineering.* 97(2):560-572. <https://doi.org/10.1002/cjce.23357>

7. DARABI, H.; ZOMORODIAN, A.; AKBARI, M.H.; LORESTANI, A.N. 2015. Design a cabinet dryer with two geometric configurations using CFD. *Journal of Food Science and Technology*. 52(1):359-366. <https://doi.org/10.1007/S13197-013-0983-1>
8. DASORE, A.; KONIJETI, R. 2019. Numerical simulation of air temperature and air flow distribution in a cabinet tray dryer. *International Journal of Innovative Technology and Exploring Engineering*. 8(11):2278-3075. <https://doi.org/10.35940/ijitee.K1787.0981119>
9. DEFRAEYE, T. 2014. Advanced computational modelling for drying processes - A review. *Applied Energy*. 131:323-344. <https://doi.org/10.1016/J.APENERGY.2014.06.027>
10. ESPARZA E., J.; GRISALES M.J., F.; PÉREZ, S.F., J.; ORDÓÑEZ S.L., E.; LOBATÓN G.H., F. 2019. Influence of the thermal conductivity of air on the moisture homogeneity of a tray dryer. *International Journal of Heat and Technology*. 37(1):322-326. <https://doi.org/10.18280/IJHT.370138>
11. FIGIEL, A.; MICHALSKA, A. 2017. Overall quality of fruits and vegetables products affected by the drying processes with the assistance of vacuum-microwaves. *International Journal of Molecular Sciences*. 18(1):71. <https://doi.org/10.3390/IJMS18010071>
12. GHOLAMZADEHDEVIN, M.; PAKZAD, L. 2019. Hydrodynamic characteristics of an activated sludge bubble column through computational fluid dynamics (CFD) and response surface methodology (RSM). *The Canadian Journal of Chemical Engineering*. 97(4):967-982. <https://doi.org/10.1002/CJCE.23335>
13. HANDAYANI, S.U.; YOHANA, E.; TAUVIQIRRAHMAN, M.; RAHMAN, A.G.; YULIANTO, M.E.; CHOI, K.H. 2023. Performance improvement of continuous horizontal fluidised bed dryer based on computational fluid dynamics. *Results in Engineering*. 17:100972. <https://doi.org/10.1016/J.RINENG.2023.100972>
14. KHATIR, Z.; THOMPSON, H.; KAPUR, N.; TOROPOV, V.; PATON, J. 2013. Multi-objective Computational Fluid Dynamics (CFD) design optimisation in commercial bread-baking. *Applied Thermal Engineering*. 60(1-2):480-486. <https://doi.org/10.1016/J.APPLTHERMALENG.2012.08.011>
15. LECORVAISIER, E.; DARCHE, S.; DA SILVA, Z.E.; DA SILVA, C.K.F. 2010. Theoretical model of a drying system including turbulence aspects. *Journal of Food Engineering*. 96(3):365-373. <https://doi.org/10.1016/j.jfoodeng.2009.08.008>
16. MARGARIS, D.P.; GHIAUS, A.G. 2006. Dried product quality improvement by air flow manipulation in tray dryers. *Journal of Food Engineering*. 75(4):542-550. <https://doi.org/10.1016/J.JFOODENG.2005.04.037>
17. MANSOUR, M.; KHOT, P.; THÉVENIN, D.; NIGAM, K.D.P.; ZÄHRINGER, K. 2020. Optimal Reynolds number for liquid-liquid mixing in helical pipes. *Chemical Engineering Science*. 214:114522. <https://doi.org/10.1016/J.CES.2018.09.046>
18. NDISYA, J.; MBUGE, D.; KULIG, B.; GITAU, A.; HENSEL, O.; STURM, B. 2020. Hot air drying of purple-speckled Cocoyam (*Colocasia esculenta* (L.) Schott) slices: Optimisation of drying conditions for improved product quality and energy savings. *Thermal Science and Engineering Progress*. 18:100557. <https://doi.org/10.1016/J.TSEP.2020.100557>
19. NEMA, P.K.; PAL KAUR, B.; MUJUMDAR, A.S. 2015. *Drying technologies for foods: Fundamentals and applications*. New India Publishing Agency. 374p.
20. PARPAS, D.; AMARIS, C.; TASSOU, S.A. 2018. Investigation into air distribution systems and thermal environment control in chilled food processing facilities. *International Journal of Refrigeration*. 87:47-64. <https://doi.org/10.1016/J.IJREFRIG.2017.10.019>
21. PRECOPPE, M.; JANJAI, S.; MAHAYOTHEE, B.; MÜLLER, J. 2015. Batch uniformity and energy efficiency improvements on a cabinet dryer suitable for smallholder farmers. *Journal of Food Science and Technology*. 52:4819-4829. <https://doi.org/10.1007/S13197-014-1544-Y>
22. QADER, B.S.; SUPENI, E.E.; ARIFFIN, M.K.A.; TALIB, A.R.A. 2019. RSM approach for modeling and optimization of designing parameters for inclined fins of solar air heater. *Renewable Energy*. 136:48-68. <https://doi.org/10.1016/J.RENENE.2018.12.099>
23. SABAREZ, H.T. 2016. Airborne Ultrasound for Convective Drying Intensification. In: Knoerzer, K.; Juliano, P.; Smithers, G. (eds). *Innovative food processing technologies: extraction, separation, component modification and process intensification*. Woodhead Publishing Series in Food Science, Technology and Nutrition. p.361-386. <https://doi.org/10.1016/B978-0-08-100294-0.00014-6>
24. SALAMI, P.; AHMADI, H.; KEYHANI, A.; SARSAIFEE, M. 2010. Strawberry post-harvest energy losses in Iran. *Researcher*. 2(4):67-73.
25. SAMRUAMPHIANSKUN, T.; PIUMSOMBOON, P.; CHALERMSINSUWAN, B. 2012. Effect of ring baffle configurations in a circulating fluidized bed riser using CFD simulation and experimental design analysis. *Chemical Engineering Journal*. 210:237-251. <https://doi.org/10.1016/J.CEJ.2012.08.079>
26. SUBRAMANIAM, P. 2016. *The stability and shelf life of food*. Second edition. Woodhead Publishing Series in Food Science, Technology and Nutrition. 590p. <https://doi.org/10.1016/C2015-0-06842-3>

27. TZEMPELIKOS, D.; VOUIROS, A.; BARDAKAS, A.; FILIOS, A.; MARGARIS, D. 2012. Analysis of air velocity distribution in a laboratory batch-type tray air dryer by computational fluid dynamics. *International Journal of Mathematics and Computers in Simulation*. 6(5):413-421.
28. VARGAS, N.A.; CAICEDO, M.; MARTÍNEZ-CORREA, H.A.; LOBATÓN, H.F. 2018. Drying uniformity analysis in a tray dryer: An experimental and simulation approach. *Advance Journal of Food Science and Technology*. 233-238. <https://doi.org/10.19026/AJFST.14.5901>